

Chapter

Plasmonic Enhanced Photoluminescence of Lanthanide-Doped Upconversion Nanoparticles

Caroline Friedersdorf and Hao Jing

Abstract

Lanthanide-doped upconversion nanoparticles (UCNPs) have garnered great interest in recent decades due to their unique ability to convert near-infrared excitation into ultraviolet or visible emission. Advancements in understanding this phenomenon have been advantageous to expanding the wide range of applications for UCNPs, from biomedicine to anticounterfeiting to renewable energy. To date, the biggest limitation in further progressing the applications of UCNPs is their inherently low efficiency of energy transfer and therefore low efficiency of upconversion photoluminescence. Recent developments have shown promise in utilizing plasmonic nanoparticles to enhance the upconversion efficiency of UCNPs. The plasmonic enhanced luminescence can occur through either selective enhancement of UCNP emission or broad enhancement of UCNP excitation. In this chapter, we present a comprehensive overview into recent advancements in plasmonic modulated enhancement of lanthanide-doped upconversion nanoparticles, addressment of current challenges, and future opportunities.

Keywords: upconversion nanoparticles, plasmonic nanoparticles, lanthanide, nanophotonics, quantum dots

1. Introduction

Lanthanide-doped upconversion nanoparticles (UCNPs) have the rare ability to convert two or more lower-energy (near-infrared) photons into one higher-energy (ultraviolet (UV) or visible) photon. This non-linear upconversion process is an anti-Stokes emission experimentally discovered by François Auzel in the 1960s [1]. The optical properties of UCNPs are highly tunable and depend greatly on the chemical composition of the nanoparticle.

The basic components of UCNPs are the host matrix material, sensitizer ions, and activator ions (**Figure 1a,b**) [2]. The host matrix must be favorable for housing the dopant ions, have low phonon energy (to minimize non-radiative decay), be chemically inert, and have high chemical stability [4, 5]. With these parameters in

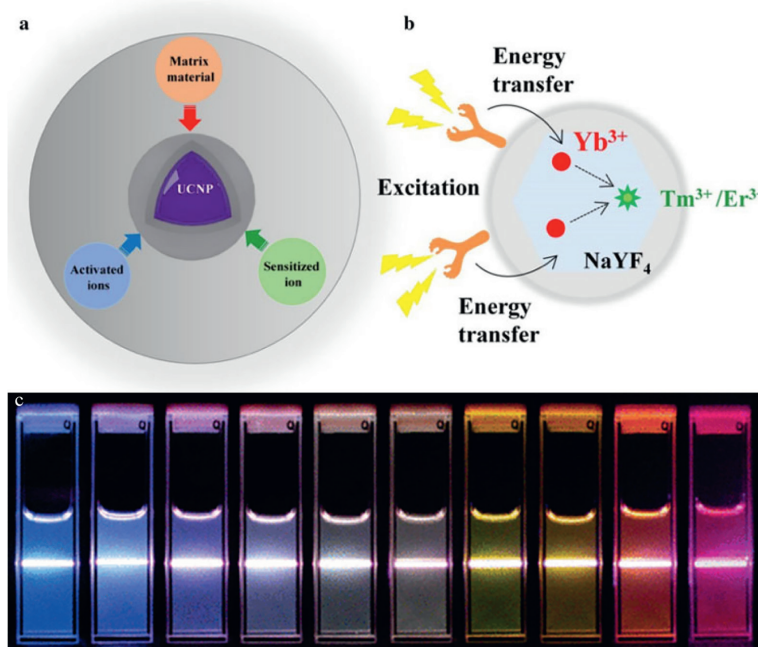


Figure 1.

The (a) basic components and (b) illustration of the energy transfer mechanism of UCNPs. (c) Upconversion emission of samples of varying sensitizer/activator pairs at varying concentrations excited at 980 nm (Reprinted with permission from Ref. [2, 3]. Copyright BioMed Central and American Chemical Society).

mind, NaXF_4 is an example of commonly chosen host matrix material, especially NaYF_4 , due to yttrium's unique energy level structure that allows for intra-4f or 4f-5d transitions and therefore sharp luminescence emissions [2, 4]. The sensitizer ions absorb the near-infrared (NIR) excitation source and transfer the energy to the activator ions for upconversion to UV or visible emission [2]. Ytterbium (Yb^{3+}) is a popular sensitizer choice due to its sufficiently large absorption cross-section at 980 nm and usually maintaining only one excited 4f state, allowing for efficient energy transfer to adjacent activator ions that have closely matched intermediate-excited state, such as erbium (Er^{3+}) and thulium (Tm^{3+}) [2, 6, 7]. Neodymium (Nd^{3+}) can also be chosen as a sensitizer due to its large absorption cross-section at 808 nm (which avoids the absorption of water and tissue heating seen with Yb^{3+}) but is less efficient than Yb^{3+} due to having multiple 4f excited state options [8–10]. Er^{3+} and Tm^{3+} are popular activator choices due to their long-lived intermediate energy states and ability to excite from the intermediate state to higher state for UV or visible emission, as well as their spectral tuning capabilities [2, 11]. Combining different sensitizer and activator pairs at varying concentrations allows for the ability to fine tune the UCNPs emission wavelength/color across the ultraviolet and visible spectrum (**Figure 1c**) [3, 12, 13].

Although there are numerous well studied techniques associated with the synthesis of lanthanide-doped UCNPs, a known significant limitation of current techniques is the consistent low efficiency of energy transfer, resulting in low yield of upconverted luminescence. Increasing the yield of upconverted luminescence would improve the practicality of using UCNPs for their potential widespread applications

ranging from cancer treatments, anticounterfeiting, bioimaging, enhanced latent fingerprint analysis, enhanced solar cells, and more [2, 14–18].

2. Lanthanide-doped upconversion mechanisms

It is generally accepted that the upconversion process of lanthanide-doped UCNPs occurs most commonly through the following three energy transfer mechanisms: excited state absorption (ESA), energy transfer upconversion (ETU), and photon avalanche (PA). Additional, less efficient mechanisms, include cooperative sensitization upconversion (CSU) and energy migration-mediated upconversion (EMU). All mechanisms include the sequential absorption of two or more photons and result in one higher-energy photon emitted. Trivalent lanthanide ions have 4f energy levels that are shielded by their filled 5s and 5p electronic shells, resulting in longer excited state lifetimes and weak electron phonon interactions, allowing the double excitation (with sharp bands) seen in these mechanisms to occur [19–22]. The general energy diagrams of the five mechanisms are visualized below (Figure 2) [23].

ESA is a multi-step excitation, where successive pump photons are absorbed by a single ion, first to a metastable level and then to a higher-lying state, resulting in upconversion emission from the higher-lying state to ground state [19, 24]. ETU differs from ESA in that the energy transfer occurs between two ions. In ETU, two neighboring ions absorb pump photons to the metastable level, then one species (sensitizer) transfers (non-radiative) its energy to the other (activator), promoting the activator ion to the higher-lying state, again resulting in upconversion emission from the transition of higher-lying state to ground state [24, 25]. PA also involves two ions, but in this case one ion has a pump intensity above a threshold value, that is triggered by a neighboring ion with a pump photon in the metastable level to induce ESA in the first ion [24, 25]. CSU is a similar mechanism to ETU with the difference being CSU does not involve the activator having a long-lived intermediate energy state, resulting in inefficient upconversion by this mechanism [23]. EMU differs from the other mechanisms in that it involves at least four ions (sensitizer, accumulator, migrator, and activator) where upon excitation, the ETU process occurs using two ions, this energy is then transferred to the third ion, which is then transferred to the fourth ion for emission [26–28]. Of the mentioned mechanisms, ETU is the most efficient upconversion mechanism for lanthanide-doped UCNPs [1, 4, 29].

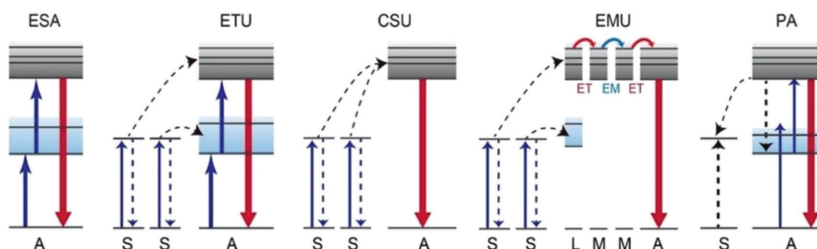


Figure 2.
 Basic energy transfer mechanisms for ESA, ETU, CSU, EMU, and PA (Reprinted with permission from Ref. [23].
 Copyright IOPScience).

3. Plasmon enhanced upconversion luminescence

3.1 Localized surface plasmon resonance of noble metal nanoparticles

Localized surface plasmon resonance (LSPR) is a phenomenon that occurs when noble metal nanoparticles interact with light, where the nanoparticle is smaller than the incident wavelength. Due to the noble metal nanoparticle being smaller than the incident wavelength of light, the oscillating electric field of the incident light interacts with the nanoparticle surface electrons to result in their collective oscillation (a plasmon) with respect to the fixed positive ions with a frequency (Eq. (1)) known as the LSPR (**Figure 3**) [30–32]. The term surface plasmons refers to the fact that the electrons on the surface are the most relevant in terms of collective oscillation due to the limited penetration depth of an electromagnetic wave on a metal surface [33, 34]. The surface plasmon is excited when the frequency of the incident light and surface plasmon are the same. When this occurs, the nanoparticles absorb the incident light, and some of the photons will undergo scattering (released in all directions at the same frequency and energy) while others will undergo absorption (converted into phonons/vibrations of the lattice) to culminate in an optical extinction spectrum [34, 35].

$$\omega_B = \sqrt{\frac{4\pi e^2 n}{m e}} \quad (1)$$

Equation (1) the plasmon frequency (ω_B) with respect to electron charge (e), number density of electrons (n), and effective mass of electrons (m) [31, 34].

Gold and silver are the most common materials used to support surface plasmons, as both have plasmonic properties that are highly tunable [36, 37]. Gold nanoparticles are particularly common due to their high stability, biocompatibility, surface functionality, cost effective fabrication, ease of use and interpretation, and high sensitivity that allows them to be utilized for widespread applications [38–41]. It is well established that the size, shape, material, aspect ratio, physical dimensions, and environment (refractive index) of the plasmonic nanoparticles can be altered to fine tune the plasmon spectral peak shift and LSPR sensitivity [42, 43].

Shapes of plasmonic nanoparticles can vary widely, from nanospheres to nanorods, nanocubes, nanobipyramids, nanoprisms, nanostars, nanocages, and more [42, 44–49]. Adjusting the shape and refractive index of the nanoparticle can

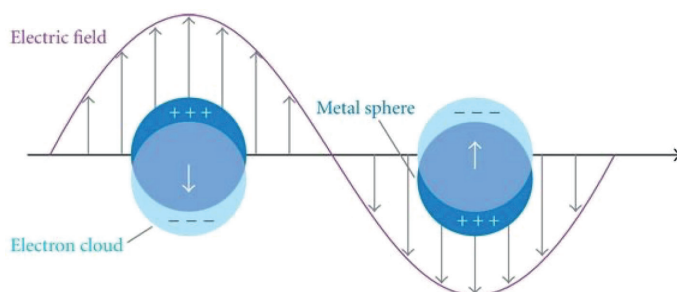


Figure 3. Illustration of localized surface plasmon resonance (Reprinted with permission from Ref. [30]. Copyright American Chemical Society).

tune the location and width of the LSPR peak, change the number of LSPR peaks, adjust their scattering and absorption cross-sections, as well as affect the strength of the surrounding electric field based on properties such as aspect ratio, size, tip sharpness, and whether the shape is isotropic or anisotropic. This is due to changes in how absorption versus scattering contribute to extinction and consistent versus variation of the incident electric field across the surface of the particle [42, 43, 50]. The core material (gold, silver, etc.) of the nanoparticle can be adjusted to fine tune the plasmon spectral peak shift due to the different core materials having different dielectric constants (real and imaginary parts), electron density, and concentration, among other factors [42, 43, 51–53].

A similar phenomenon to LSPR also occurs for doped semiconductor nanoparticles, with the difference being the collective oscillation is of free holes in the valence band, as opposed to the collective oscillation of free electrons in the conduction band seen for noble metal nanoparticles [54]. Doped semiconductor nanoparticles often exhibit LSPR peaks in the NIR or mid-infrared (MIR) regions due to their lower carrier density when compared to noble metal nanoparticles, and p-type semiconductors are tunable in relation to carrier density, oxidative generation, and reductive filling of copper vacancies (specifically for copper chalcogenide nanoparticles) [55–58]. But the LSPR peaks of doped semiconductor nanoparticles are typically not as strong or well-defined as those of noble metal nanoparticles [34].

3.2 Modulation of photoluminescence of UCNPs with plasmonic nanoparticles

Plasmonic nanoparticles can be exploited in two different ways to enhance the upconversion efficiency of UCNPs. The first is to selectively enhance the emission of the UCNPs through plasmonic modulation by matching the emission profile of the UCNPs to the LSPR band of the plasmonic nanoparticle (**Figure 4a**). Such enhancement has been achieved *via* either the Purcell effect (an increase in the local density of photonic states at the emission wavelength) or the improved absorption efficiency owing to the plasmon-induced local-field confinement. The second is the broad enhancement of photoluminescence of UCNPs *via* amplification of the excitation field when the surface plasmon resonates with the excitation wavelength (**Figure 4a**).

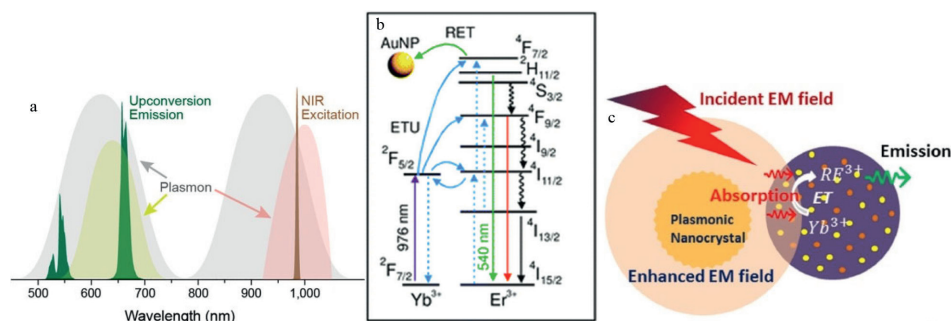


Figure 4. Illustration of (a) the overlap between excitation or emission of UCNPs with LSPR bands of plasmonic nanoparticles, (b) an energy-level diagram of the UCNP ETU mechanism (Yb³⁺ sensitizer; Er³⁺ activator) with a pathway demonstrating the energy transfer to a gold nanoparticle, and (c) the enhanced electromagnetic field from a plasmonic nanoparticle resulting in enhanced UCNPs cross-section absorption and UCNPs emission (Reprinted with permission from Ref. [59–61]. Copyright American Chemical Society, Royal Society of Chemistry, and Elsevier).

3.3 Plasmon enhanced emission of UCNPs

The selective enhancement of the emission of UCNPs is typically done by coupling UCNPs to plasmonic nanoparticles with overlapping optical properties, such that the emission profile of the UCNPs overlaps with the LSPR band of the coupled plasmonic nanoparticle. The exact mechanism of this surface-plasmon upconversion coupling has yet to be determined, but it is generally agreed that the Purcell effect contributes to the plasmon-enhancement of specific emissions of UCNPs [62]. According to Fermi's golden rule, the radiative decay rate is dependent on the density of states (both photon and electronic states) (Eq. (2)), and a surface plasmon introduces an increased photon density of states, enhancing the radiative decay rate (can be predicted from the dyadic Green function (Eq. (3))), and therefore enhancing the upconversion photoluminescence [59, 63, 64]. It is currently still debated if the Förster energy transfer rate is dependent on density of states, which would allow for plasmon-enhanced Förster energy transfer and enhanced upconversion photoluminescence [63].

$$W = \frac{2\pi}{\hbar} |\psi_f H_{\text{int}} \psi_i| \rho(\omega_f - \omega_i) \quad (2)$$

Equation (2) the rate (W) of an electronic transition with respect to the initial and final states (ψ_i and ψ_f), density of states (ρ), and initial and final energy ($\hbar\omega_i$ and $\hbar\omega_f$) [63].

$$\rho(r_0, \omega) = \frac{6\omega}{\pi c^2} \left[\hat{n}_d \cdot \text{Im} \left\{ \tilde{G}(r_0, r_0, \omega) \right\} \cdot \hat{n}_d \right] \quad (3)$$

Equation (3) the density of states (ρ) with respect to the dyadic Green function, the unit vector (\hat{n}_d) along the direction of the induced dipole moment, the position of the emitter (r_0), and plasmon frequency (ω) [63].

Since the emission profile of UCNPs of different compositions will vary, the plasmonic nanoparticles must be synthesized with the correct morphology to match the specific UCNP emission profile. Additionally, the size of the plasmonic nanoparticles and the distance between the coupled plasmonic nanoparticles and UCNPs is vital as to whether the plasmonic nanoparticles will enhance or quench the UCNP emission.

Typically, direct contact (or short distance) of the plasmonic nanoparticle with the UCNP will result in quenching the upconversion luminescence [61]. This is due to efficient non-radiative energy transfer from UCNP to the metal, increasing the rate of non-radiative decay (the rate of which can be calculated from the ohmic loss in the environment for the field emitted from a radiated dipole (Eq. (4))), and quenching the upconversion photoluminescence (**Figure 4b**) [60, 63]. Therefore, a spacer shell is often used to increase and optimize the distance between the two types of particles to result in upconversion enhancement, rather than quenching [61, 65, 66].

$$\frac{W_{\text{nr}}}{W_0} = \frac{1}{P_0} \frac{1}{2} \int_V \text{Re}[j^* \cdot E] dV \quad (4)$$

Equation (4) the additional nonradiative decay rate (W_{nr}) with respect to the free space decay rate (W_0), the radiation rate of a classical dipole (P_0), and the integration over the metal volume with regards to the current density induced by the emitted field (j), and the field emitted by the dipole emitter (E) [63].

3.4 Plasmon enhanced excitation of UCNPs

The broad enhancement of the excitation of UCNPs is typically done by coupling UCNPs to plasmonic nanoparticles with overlapping optical properties, such that the excitation profile of the UCNPs overlaps with the LSPR band of the coupled plasmonic nanoparticle. While enhancing the emissions of UCNPs is specific to the wavelength each type of UCNP emits, enhancing the NIR excitation of UCNPs is a broad approach that could be utilized on all UCNPs. Plasmonic nanoparticles with a LSPR band around in the NIR region can create localized enhanced electric fields upon excitation from the collective oscillation of free electrons, concentrating the incident field and enhancing UCNP cross-section absorption, resulting in enhanced upconversion photoluminescence (**Figure 4c**) [60, 61]. The localized enhanced electric field effect is typically most strongly seen in plasmonic nanoparticles with sharp corners or edges, such as nanobipyramids [46, 67, 68]. Although the modified localized electric field can be exploited to enhance the upconversion efficiency of UCNPs, when the two particle types are in too close proximity to one another, it can also decrease the rate of radiative emission and accelerate the rate of non-radiative relaxation by increasing the transition from intermediate state to ground state, further establishing the importance of controlling the distance between particles [65, 69].

4. Select recent publications on plasmon enhanced upconversion luminescence

4.1 Enhanced emission of UCNPs through coupling with gold nanoparticles

Gold nanoparticles are a popular choice to selectively enhance the emission of UCNPs due to their highly tunable LSPR bands in the visible spectrum [60, 70, 71]. Gold nanospheres in particular typically have a peak LSPR wavelength between 515 and 570 nm (depending on their diameter), making them preferable to couple with UCNPs with optically complimentary peak emissions in the green visible region. Mendez-Gonzalez et al. utilized gold nanospheres coupled with UCNPs to determine the optimal gold nanoparticle size and optimal silica shell thickness on UCNPs to optimize both UCNP luminescence quenching and enhancement (both having their own biomedical and other applications) [60]. This study highlights the importance that the size of the plasmonic nanoparticle and the distance between the coupled plasmonic nanoparticles and UCNPs have on whether quenching or enhancement of UCNP emission occur.

The researchers grew a silica shell on the UCNPs with an amine group to allow for adsorption of the gold nanospheres [60]. Growing a silica shell of a particular size on the UCNPs also allowed for the control to set a minimum distance between the gold nanospheres and UCNPs. The researchers found a silica shell thickness of 3.8 nm to be optimal for the quenching and enhancement experiments [60]. Regarding the size of the plasmonic nanoparticles, it was found that as the size of the gold nanospheres was increased (from 4 nm to 36 nm), there was a reduction in the quenching effect of the gold nanosphere on the UCNP (18 nm with a 3.8 nm silica shell) [60]. As the gold nanosphere size was further increased (41+ nm), there was a luminescence enhancement observed (instead of quenching), and peak luminescence enhancement occurred when 66 nm gold nanospheres were coupled to the UCNPs [60].

These experimental findings were theoretically reproduced to demonstrate how the Purcell effect and non-radiative resonance energy transfer compete with one another to result in either quenching or enhancement of luminescence to dominate based on gold nanosphere size and silica shell size (**Figure 5**) [60].

4.2 Enhanced excitation of UCNPs through coupling with gold nanoparticles

Not only can gold nanoparticles be used to enhance the emission of UCNPs, but they can be used to broadly enhance the excitation of UCNPs as well [69, 72, 73]. Gold nanorods and nanobipyramids have a tunable peak LSPR wavelength in the NIR region that can optically compliment the absorbance wavelength of UCNPs. Liu et al. utilized gold nanorods to theoretically simultaneously enhance both the excitation and emission of UCNPs [69]. Since gold nanorods are anisotropic, they exhibit two main characteristic LSPR peaks (associated with the longitudinal and transverse electron oscillations).

In the case of this study, the gold nanorods were simulated to have an aspect ratio to allow for a strong LSPR peak (longitudinal) around 980 nm and another LSPR peak (quadruple) around 650 nm (**Figure 6**) [69]. The gold nanorods also had a very weak transverse LSPR around 540 nm (**Figure 6**) [69]. This is optically complementary to commonly synthesized UCNPs that have an excitation wavelength of 980 nm and two main emission peaks around 540 nm and 650 nm (**Figure 6**) [69]. This allows for enhanced excitation due to electric field enhancement from the longitudinal LSPR of the gold nanorod, as well as enhanced emissions that are distant dependent due to the quadruple and transverse LSPRs of the gold nanorod. If applied, the results

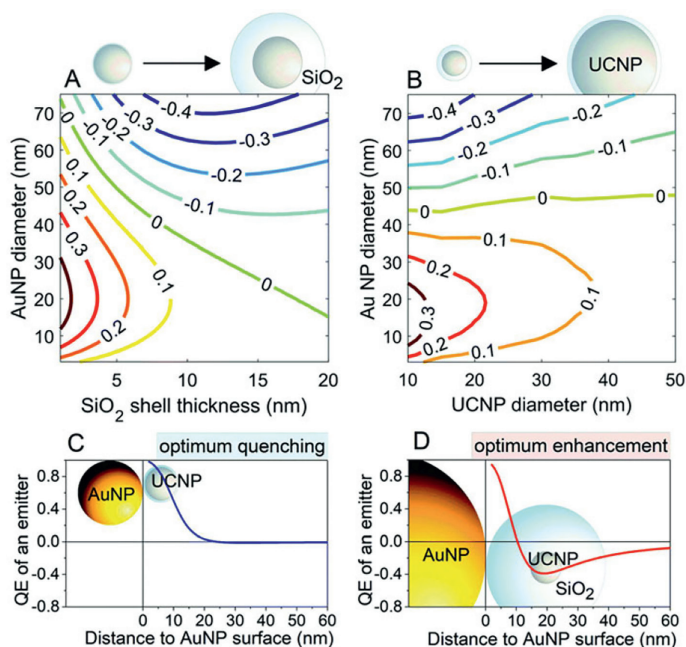


Figure 5. Simulated plots of quenching or enhancement efficiency as a function of gold nanosphere diameter, silica shell thickness, and UCNP diameter (Reprinted with permission from Ref. [60]. Copyright Royal Society of Chemistry).

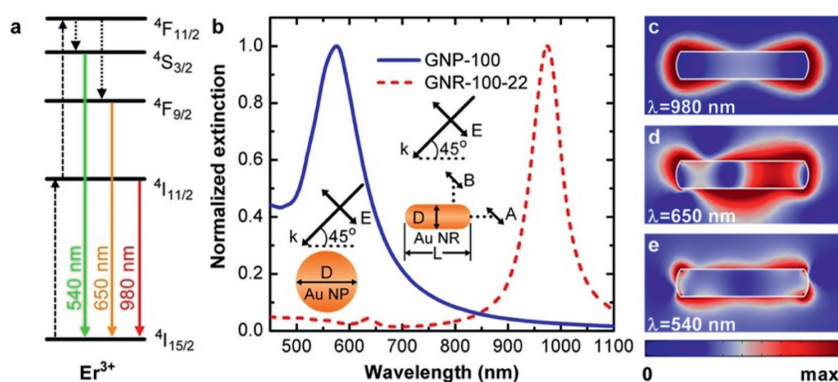


Figure 6. Simulated (a) energy-level schematic for Er^{3+} doped UCNP, (b) extinction spectra of gold nanospheres versus proposed gold nanorods, and electron field distribution in the gold nanorod wavelengths of (c) 980 nm, (d) 650 nm, and (e) 540 nm (Reprinted with permission from Ref. [69]. Copyright Nature).

modeled can theoretically result in a maximum upconversion enhancement factor of 120-fold for the 650 nm emission wavelength and 160-fold for the 540 nm emission wavelength at separation distances between nanoparticles ranging from 5 to 15 nm [69]. Although this study was based on numerical calculations and physical models rather than experimental studies, it still highlights the importance to precisely control the separation distance between plasmonic and upconversion nanoparticles, as well as highlights the potential for significant plasmon-modulated enhanced upconversion luminescence [69].

4.3 Enhanced excitation of UCNP through controlled growth of gold nanoshell

Although there are numerous publications on the coupling of gold nanoparticles with UCNP for enhanced upconversion luminescence, a minor limitation to these studies is that most utilize some form of spacer shell to set the distance between plasmonic and upconversion nanoparticles. Although this sets a minimum distance between particles (importantly to prevent the plasmonic modulated quenching seen at too short of distances between particles), not all particles will couple with each other, and some particles will couple further away than the length of the spacer shell. A solution that would allow for a more controlled and exact distance between particles would be to grow a spacer shell on the UCNP followed by the growth of a gold shell. Not only does this allow for more precise studies on the distance dependence between UCNP and gold nanoparticle and its role on enhancement or quenching of photoluminescence, but it would also theoretically allow all UCNP to be surrounded by a gold shell (rather than depending on the molar ratios of upconversion to gold nanoparticle).

Priyam et al. broadly enhanced UCNP through coating UCNP with a gold nanoshell that has an LSPR peak in the NIR region complimentary to the excitation wavelength of the UCNP (Figure 7) [74]. In this case, a silica shell was coated on the UCNP first to act as a tunable distance spacer shell between the UCNP and gold nanoshell (Figure 7) [74]. With the growth of the gold nanoshell, two main factors were considered. The first factor was that it must be thin enough to allow the luminescence from the UCNP to pass through [74]. The second factor was that the spacer shell needs to separate the UCNP from the gold shell [74]. These factors come

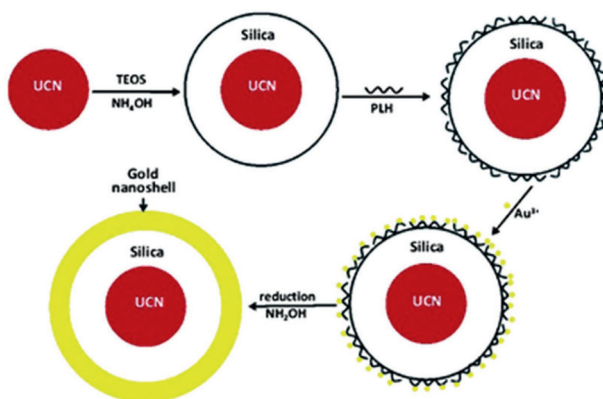


Figure 7.

Schematic of the growth of a silica shell on the UCN followed by the growth of the gold nanoshell (Reprinted with permission from Ref. [74]. Copyright Royal Society of Chemistry).

with limitations, such as the way gold shells are typically grown would result in too thick of a shell that would block upconversion luminescence [74]. For this reason, the authors chose to use a silica shell as the spacer shell due to its easily tunable thickness on UCNP and study the effect of various thicknesses of gold shell [74].

The study demonstrated the importance of the thickness of the gold nanoshell (and therefore the LSPR peak) on whether enhanced or quenched luminescence occurred. With a gold nanoshell thickness of 8–9 nm that possessed a maximum LSPR peak at 580 nm, it was found that luminescence was quenched by approximately 80% [74]. As the gold nanoshell thickness was decreased to 3 nm and the maximum LSPR peak was at 900 nm, there was no longer quenching observed, and instead there was substantial enhancement of all three UCN emission peaks due to the electric field enhancement [74]. In addition to the substantial enhancement of the upconversion luminescence, the gold nanoshell also demonstrated additional functionalities, such as plasmon scattering, which also made the hybrid-nanoparticle system useful for upconversion fluorescence imaging and darkfield light scattering imaging, expanding on potential bioimaging applications [74].

4.4 Enhanced emission of UCNP through coupling with silver nanoparticles

Other noble-metal nanoparticles, including silver nanoparticles, can also be used to selectively enhance the emission of UCNP, although this area has been less explored in the literature compared to the use of gold nanoparticles [75–77]. Silver nanospheres typically have a peak LSPR wavelength between 400 and 500 nm (depending on their diameter), making them preferable to couple with UCNP with optically complimentary peak emissions in the blue visible region. More recent research explores upconversion nanocomposites, combining multiple nanomaterials to enhance the efficiency of upconversion luminescence [75]. Liu et al. designed upconversion nanocomposites consisting of UCNP, perovskite quantum dots (PeQDs), and silver nanoparticles [75]. It has been well established that combining PeQDs and UCNP results in a sizable increase in the upconversion luminescence of PeQDs, and that noble metal nanoparticles can also enhance the photoluminescence emission efficiency of PeQDs, but the literature is lacking in the area of how localized plasmon resonance effects the upconversion luminescence of nanocomposites (such as UCNP/PeQDs nanocomposites) [75].

In this study, the silver nanoparticles were synthesized to have a peak LSPR band around 450 nm, overlapping with the blue light emission of the synthesized UCNP [75]. The UCNP/PeQDs nanocomposites were successfully coupled to the silver nanoparticles to result in an approximately six-fold enhancement of upconversion emission (**Figure 8**) [75]. To further confirm plasmon enhanced luminescence was occurring, the authors found that the addition of the silver nanoparticles resulted in reduced photoluminescence lifetimes of the nanocomposites, indicative that the plasmons accelerate the radiated decay rate of the UCNP for enhanced photoluminescence emission efficiency (**Figure 8**) [75]. Again, the distance between the plasmonic nanoparticle and UCNP/PeQDs nanocomposites was found to be vital for enhancement to occur, and in this case the distance where enhancement was observed was 5–8 nm [75]. Additionally in this study, the optimal molar ratio of nanocomposite: silver nanoparticle was studied and was experimentally determined to be 1:0.5 [75]. Importantly, it was found that no significant enhancement was observed for the other ratios studied, signifying the importance of reporting the molar ratio for similar studies [75].

4.5 Enhanced excitation of UCNP through coupling with silver nanoparticles

Similar to gold nanoparticles, silver nanoparticles or nanosystems can also be used to broadly enhance the excitation of UCNP as well [78–80]. Lu et al. deposited water soluble UCNP on silver nanograting that had a peak LSPR wavelength complimentary to the absorbance wavelength of the UCNP [78]. The UCNP underwent surface modification (ligand exchange of oleic acid to

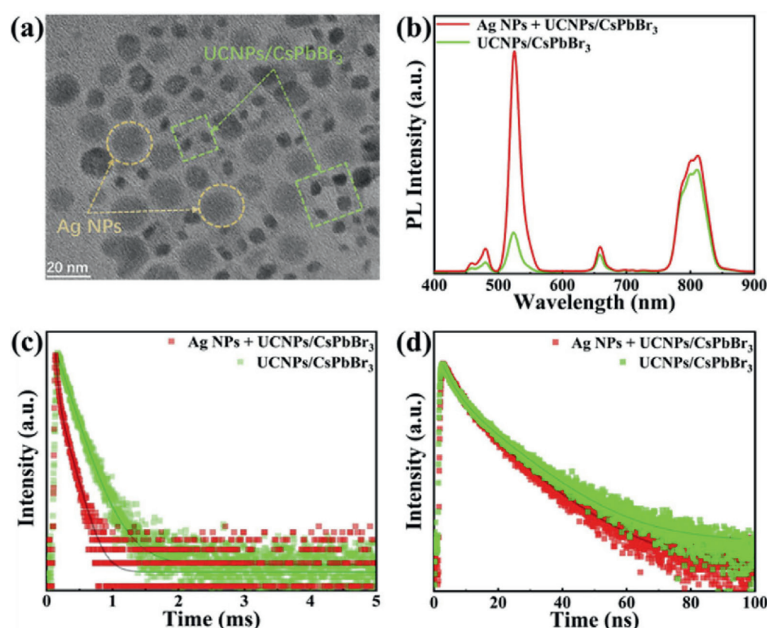


Figure 8. (a) TEM imaging of the UCNP/PeQDs nanocomposites coupled to the silver nanoparticles. A comparison before (green) and after (red) coupling the UCNP/PeQDs nanocomposites with the silver nanoparticles for the (b) photoluminescence spectra, (c) time-resolved decay curve (monitored at 481 nm), and (d) time-resolved decay curve (monitored at 526 nm) (Reprinted with permission from Ref. [75]. Copyright Optica Publishing Group).

poly(maleicanhydride-alt-1-octadecene) (PMAO)) to become water-soluble, and the silver nanograting structure was fabricated using nanoimprint lithography (**Figure 9**) [78]. The UCNP were then deposited on the silver nanograting using a layer-by-layer approach [78]. Compared to the UCNP deposited on a flat silver film, when deposited on the silver nanograting, there was a 16-fold increase in the green photoluminescence intensity and a 39-fold increase in the red photoluminescence intensity of the UCNP [78].

The authors demonstrated the importance of specifying the excitation conditions used in experiments. Since upconversion is a nonlinear process, it is sensitive to excitation power, and may enhance differently under different excitation power densities [78]. Under weak excitation conditions, the upconverted luminescence intensity increased quadratically with excitation power [78]. But under strong excitation conditions, the upconverted luminescence intensity increased linearly with excitation power [78]. They then went on to perform a thorough analysis of rate equations to prove that the photoluminescence enhancement was solely due to enhancement of the excitation absorption, not emission enhancement (radiative decay rate or Förster energy transfer rate) under strong excitation conditions [78]. Under weak conditions, it was found that both enhancement of excitation absorption and emission contribute, although enhancement of excitation absorption dominated [78].

4.6 Enhanced excitation of UCNP through coupling with doped semiconductors

Noble-metal nanoparticles are not the only nanoparticles that experience LSPR. Doped semiconductors experience LSPR as well (due to the collective oscillation of free holes in the valence band instead of the collective oscillation of free electrons in the conduction band seen for noble metal nanoparticles), which has garnered recent interest [81–83]. In particular, the LSPR of the doped semiconductors typically corresponds to the NIR absorbance wavelengths of UCNP. But the doped semiconductor modulated enhancement of upconversion photoluminescence has not been as thoroughly studied as that of noble-metal nanoparticles.

Ji et al. enhanced monolayer UCNP using plasmon semiconductor nanoparticles, specifically Cs_xWO_3 [81]. Cs_xWO_3 nanoparticles were chosen due to their stability, low cost, ease, and controllability, especially when compared to previously used Cu_{2-x}S nanoparticles [81]. And studying the effect of the doped semiconductor nanoparticles with monolayer UCNP allowed the authors to more precisely explore

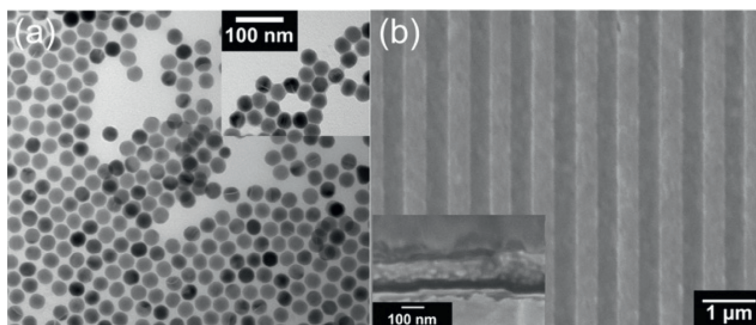


Figure 9. (a) TEM imaging of PMAO-coated UCNP and (b) SEM imaging of silver nanograting (Reprinted with permission from Ref. [78]. Copyright American Chemical Society).

the mechanism of enhancement and its narrow band near-infrared photodetection application [81]. Specifically, a $\text{Cs}_x\text{WO}_3/\text{NaYF}_4/\text{monolayer NaYF}_4:\text{Yb}^{3+}, \text{Er}^{3+}$ hybrid film was developed, where the NaYF_4 acts as a spacer between the plasmon semiconductor layer and UCNP layer (Figure 10) [81]. The spacer layer thickness, doped semiconductor concentration, upconversion nanoparticle layers, and excitation power density were optimized to result in a three-order enhancement of upconversion photoluminescence [81]. The authors then analyzed the upconversion luminescence decay time constant with and without coupling to the doped semiconductor nanoparticles and calculated the electric field intensity to confirm that excitation field amplification dominates the observed enhancement of upconversion photoluminescence [81].

4.7 Additional methods of plasmon-enhanced excitation of UCNPs

Additional methods of plasmon-enhanced excitation of UCNPs include the use of plasmonic nanocavities and photonic crystal hybrid systems [79, 84]. Plasmonic nanocavities have geometry capable of confining NIR (and visible) light to subwavelength volumes, which along with experiencing plasmon resonance, enhances optical and local field intensity [85]. In Li et al., a monodispersed metal-dielectric-metal type upconversion composite material was designed containing silver nanoparticles as the metallic core, a UCNP dielectric layer, and a silver metallic shell (Figure 11a) [79]. This sandwich style nanocavity structure can trap and localize light, where the two metal layers act as reflective mirrors [79]. In the designed composite material, this results in the generation of high-density hot carriers around the UCNP nearfield region for enhanced excitation (Figure 11b) [79]. Parameters optimized to maximize that excitation enhancement include the thickness of the outer metallic shell, UCNP diameter, and ambient refractive index to result in an UCNP photoluminescence enhancement of five orders of magnitude [79].

Photonic crystals are typically periodic structures with alternating regions of materials of different refractive indices that generate a photonic band gap, resulting in incident light reflected by the photonic crystals at specific frequencies and angles [86, 87]. Plasmonic photonic hybrid crystals possess the ability to concentrate light flow (dependent on the corresponding LSPR and photonic band gap wavelengths) to enhance local optical field intensity for enhanced excitation of UCNPs [84]. Xia et al. fabricated WO_{3-x} plasmonic photonic crystals that through electrical stimulation can have its LSPR (500–1100 nm), refractive index, and oxygen

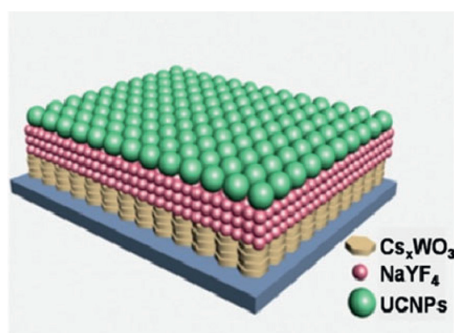


Figure 10. Illustration of the $\text{Cs}_x\text{WO}_3/\text{NaYF}_4/\text{monolayer NaYF}_4:\text{Yb}^{3+}, \text{Er}^{3+}$ hybrid film (Reprinted with permission from Ref. [81]. Copyright Elsevier).

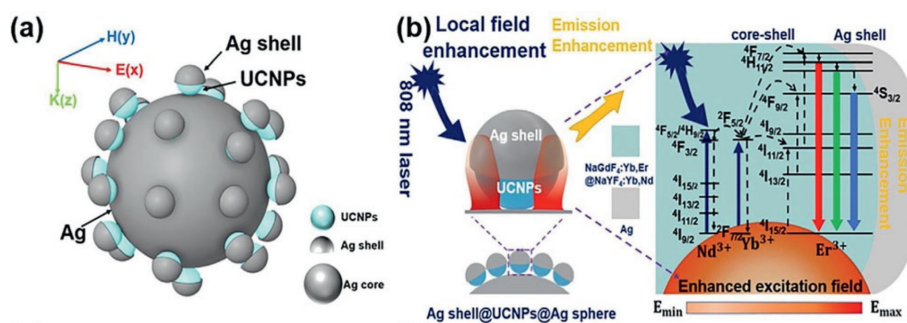


Figure 11. (a) Illustration of the monodispersed metal-dielectric-metal type upconversion composite material. (b) Schematic of the proposed enhanced UCNPs excitation mechanism (Reprinted with permission from Ref. [79]. Copyright Elsevier).

vacancy dynamically altered to result in an alternation of LSPR and photonic band gap [84]. With electrical stimulation, the reversible W^{5+} and W^{6+} alternation causes the variability in refractive index and oxygen vacancy, shifting the wavelength of the photonic band gap, and enhancing or reducing the LSPR [84]. Under negative voltages (where there is an increase in W^{5+} to W^{6+} atomic ratio for increased formation of oxygen vacancies), the refractive index is reduced, causing a decrease in reflectivity and a blue-shift of the reflection peak [84]. And a positive voltage (where there is a decrease in W^{5+} to W^{6+} atomic ratio for reduced formation of oxygen vacancies) results in an increase in refractive index, that increases reflectivity, and red-shifts the reflection peak [84]. Both lead to a change in carrier density for a tunable LSPR effect [84]. When coupled with UCNPs, a tunable enhancement of UCNPs photoluminescence of five-fold (under +1.6 V) to 26-fold (under -1.6 V) (Figure 12) was achieved [84].

4.8 Enhanced photoluminescence of UCNPs through coupling with periodic nanostructures

Periodic nanostructures, such as nanohole arrays, nanorod arrays, and nanograting have been investigated for their potential to enhance upconversion

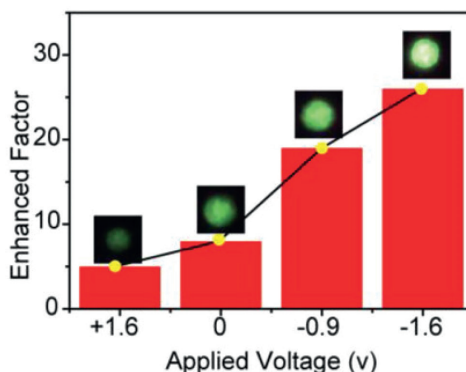


Figure 12. Upconversion photoluminescence enhancement under different applied bias voltages (Reprinted with permission from Ref. [84]. Copyright Wiley).

photoluminescence. Nanohole arrays, first studied by Ebbesen in 1998, experience both LSPR and generation of an enhanced electromagnetic field [61, 88]. Nanohole arrays contain several advantages, including their reproducible fabrication, scaling and miniaturization potential, highly tunable optical resonances, and the ability to provide a well-defined template to host UCNPs [89]. Saboktakin et al. enhanced the luminescence of UCNPs (through enhanced excitation) utilizing gold films containing nanohole arrays that produced enhanced electromagnetic fields upon excitation [89]. The gold film nanohole array was fabricated using lithographical techniques, and a “squeegee method” (**Figure 13a**) was employed to allow precise control of UCNP placement, so that each nanohole accepted only a single UCNP to maximize enhancement and reproducibility [89]. The gold film nanohole array was fine-tuned so that its resonant wavelength matched that of the excitation wavelength of the UCNPs, and the UCNP filled nanohole array experienced photoluminescence enhancements of up to 35-fold when compared to the same UCNPs in a glass nanohole array [89].

Periodic nanostructures, such as those with a regular distribution of nanorods or nanograting, have also been found to exhibit plasmonic properties that can be applied to enhance the photoluminescence of UCNPs, such as the silver nanograting structure mentioned in subsection 4.5 [78, 90]. A nanorod array can enhance the excitation of UCNPs similarly to that previously described for the nanohole array. Yin et al. fabricated a vertically aligned gold nanorod monolayer supercrystal to enhance the excitation of UCNPs through localized electromagnetic field enhancement for enhanced photoluminescence [90]. The supercrystal structure was prepared on a glass substrate using an evaporation-induced self-assembly method [90]. The synthesized supercrystal structure exhibited stronger scattering (compared to irregular aggregated gold nanorod film) which is associated with photoluminescence enhancement when coupled with UCNPs [90, 91]. The authors also demonstrated the importance of optimizing the distance between the UCNPs and the gold nanorod array to maximize enhancement and prevent quenching of photoluminescence. A MoO_3 monolayer was used a spacer between UCNPs and the gold nanorod array [90]. It was found that enhancement of photoluminescence increased as the spacer thickness increased, until maximum enhancement occurred with a MoO_3 spacer thickness

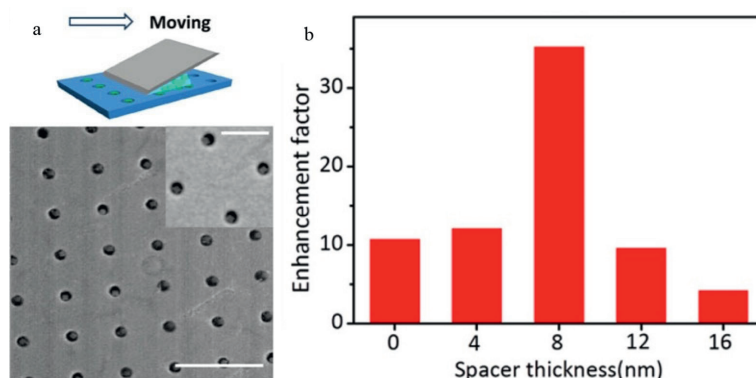


Figure 13. (a) Illustration of squeegee method used to fill nanohole array with UCNPs and SEM image of nanohole array filled with UCNPs. (b) UCNP enhancement factor as a function of spacer thickness of MoO_3 monolayer on gold nanorod array (Reprinted with permission from Ref. [89, 90]. Copyright American Chemical Society).

of 8 nm, after which a further increase in thickness lead to a decrease in enhancement of photoluminescence (**Figure 13b**) [90]. The authors also simulated the local electromagnetic field distribution of the gold nanorod array to demonstrate the uniformity in electromagnetic field amplification and that a homogeneous distribution of “hot spots” were robustly produced with as high as 113 times amplification in electromagnetic field strength [90]. Upon optimization of the above-mentioned factors, the UCNPs deposited on the supercrystal structure were found to experience photoluminescence enhancements of over 35-fold when compared to UCNPs deposited on a glass substrate [90].

4.9 Plasmonic dual enhancement of both excitation and emission of UCNPs

Most commonly, plasmonic nanoparticles are employed to separately enhance either the excitation or emission of UCNPs to result in enhanced upconversion photoluminescence. But new studies are emerging that utilize plasmonic nanoparticles or nanostructures to dually enhance both the excitation and emission of UCNPs to maximize photoluminescence enhancement [92–94]. This can be done using plasmonic nanoparticles or nanostructures that exhibit at least 2 LSPR peaks (one that corresponds to the emission wavelength and one that corresponds to the excitation wavelength of the UCNPs, such as the nanorods described in subsection 4.2) or using those that exhibit a very broad LSPR peak that encompasses both the emission and excitation wavelengths of the UCNPs.

Nanoparticles can be synthesized to exhibit a wide LSPR peak to contain both the UCNPs emission and excitation wavelengths. Xu et al. designed silver nanowire network plasmonic antenna that exhibit a single, very wide LSPR peak (350–3000 nm) to enhance both the excitation and emission of UCNPs [92]. Due to the tunability and large range of the LSPR band, the nanowire network design has the potential to broadly enhance almost all types of lanthanide-doped UCNPs, regardless of excitation or emission wavelengths. The coupling between individual nanowires within the nanowire network occurs in mostly upper-and-lower and side-by-side dimer configurations, creating broad gap plasmon regions between nanowires that can generate strong plasmon hybridization, resulting in the exhibited very wide LSPR peak [92]. Analysis (discrete dipole approximation calculation and dark-field scattering spectrum) of the nanowire network demonstrated that the plasmonic nanoparticles mostly enhanced light scattering [92]. UCNPs were deposited into the nanowire network where they were found to be densely distributed and well-integrated (**Figure 14**) [92]. In the hybrid UCNP and nanowire system, photoluminescence of UCNPs was enhanced approximately 350-fold under 1540 nm excitation and 50-fold

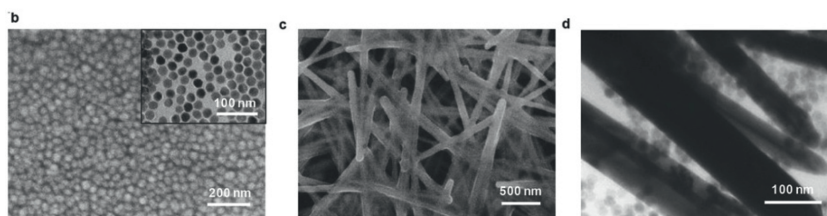


Figure 14. SEM and TEM images of the (b) UCNPs, (c) silver nanowire system, and (d) hybrid UCNP and silver nanowire system (Reprinted with permission from Ref. [92]. Copyright Wiley).

under 980 nm excitation [92]. Although the authors attributed the majority of the photoluminescence enhancement was due to excitation field enhancement, this study still opens the door for future work to further increase the emission enhancement through the Purcell effect for nanoparticles with ultrabroad LSPR peaks to maximize dual enhancement of the excitation and emission of UCNPs.

Nanoparticles can also be synthesized to exhibit two LSPR peaks that correspond to both the excitation and emission wavelengths of UCNPs. Mi et al. designed gold-copper Janus nanojellyfish to dually enhance the excitation and emission of coupled UCNPs [94]. The name “Janus” nanoparticles was first proposed by de Gennes, with Janus referring to the ancient Roman god Janus who had two faces that faced different directions, indicative of the Janis nanoparticles combining two (or more) chemically different composites into one system [94–96]. The term “jellyfish” refers to the shape of the synthesized nanoparticles. The authors used the twinned tips of gold nano-flowers as seeds, on which copper was deposited asymmetrically due to the large lattice mismatch between gold and copper (**Figure 15**) [94]. The resulting gold-copper Janus nanojellyfish has two characteristic LSPR peaks; one in visible region and one in the NIR region, associated with the gold portion and copper portion (respectively) of the nanojellyfish. These peaks could be fine-tuned to overlap with the emission and excitation wavelengths of the UCNPs by adjusting the volume of gold seeds and CuCl_2 used in the synthesis [94]. When the gold-copper Janus nanojellyfish were coupled with UCNPs, a 5000-fold enhancement of UCNP photoluminescence was observed [94]. Analysis proved that the electric field was significantly enhanced under 980 nm

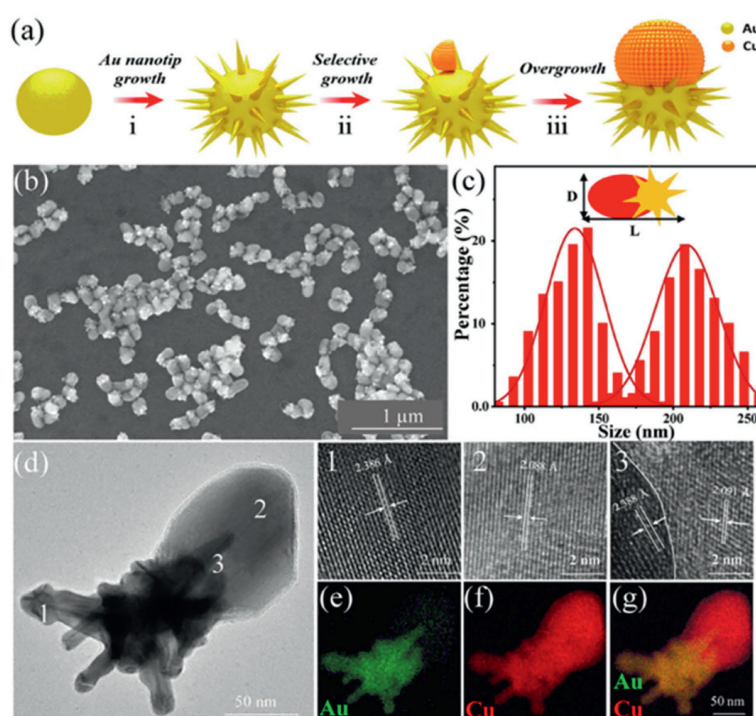


Figure 15. The (a) illustration of the synthesis pathway, (b) SEM image, (c) distribution of the diameter and length, (d) HRTEM image, and (e-g) elemental mapping images of the gold-copper Janus nanojellyfish (Reprinted with permission from Ref. [94]. Copyright Elsevier).

excitation (observed in the tips and gaps of the nanojellyfish) to result in enhanced excitation of UCNPs, as well as the quantum efficiency was enhanced to result in emission enhancement of UCNPs [94].

Additional methods of dually enhanced photoluminescence of UCNPs have recently been explored using non-metal particles [94, 97]. This includes the use of dielectric micro- or nanostructures, which are high-index particles with resonant behavior that can be used to enhance light-matter interactions, without the quenching observed for metal nanoparticles/nanostructures [97–99]. Liang et al. utilized transparent, polymeric dielectric microbeads (comprised of poly(ethylene glycol) diacrylate) (**Figure 16a** and **b**) to enhance both the excitation and emission of UCNPs through dielectric superlensing effects for up to 5 orders of magnitude photoluminescence amplification (**Figure 16c**) [98]. The microbeads acting as a superlens confine the incident light into a sub-wavelength photonic hotspot of high field intensity, that does not rely on increasing radiative emission, but instead enhances the efficiency of far-field light collection and photon-photon interactions in UCNPs under low-power incident light, through modulating the wavefront of both the excitation and emission fields of UCNPs [98]. Gong et al. further applied the idea of dielectric nanostructures in the form of a dual-resonance all-dielectric metasurface (consisting of a periodic lattice of silicon structures) (**Figure 16d**) to enhance the signal of UCNPs by 400 times (**Figure 16e**) [97]. The all dielectric metasurface enhances UCNP photoluminescence through modifying the upconversion fluorescence excitation rate (related to the near field enhancement through resonance of the excitation wavelength), the quantum efficiency (through the Purcell effect), and the collection efficiency (through acting as an antenna array that modifies the UCNP radiation pattern to result in increased efficiency of emission collection) [97]. The electric dipole

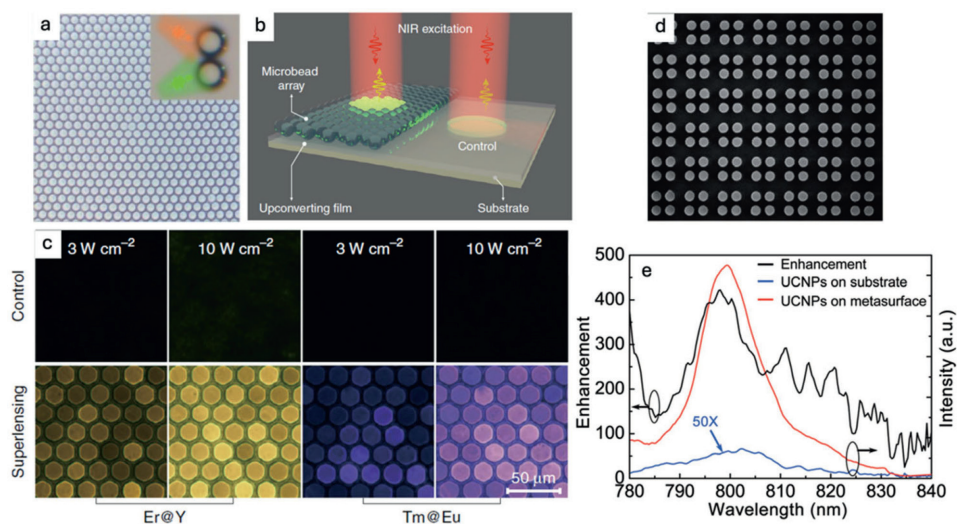


Figure 16.

(a) Photographic image of the polymeric microbeads. (b) Schematic of experimental set up. (c) Upconversion photoluminescence images of the UCNP-embedded polydimethylsiloxane film featuring dual under 980 nm excitation without (control) and with (superlensing) microbead coverage. UCNPs of interest include NaYF₄:Yb/Er@NaYF₄ (Er@Y) and NaGdF₄:Yb/Tm@NaGdF₄:Eu (Tm@Eu). (d) SEM image of a fabricated all-dielectric metasurface sample. (e) Upconversion emission spectra of UCNPs on substrate (blue) and metasurface (red) with enhancement (black) overlaid (Reprinted with permission from Ref. [97, 98]. Copyright Nature and Royal Chemistry Society).

resonance of the metasurface enhances the local excitation field, the magnetic dipole resonance of the metasurface enhances the quantum efficiency of the UCNPs, and the array of the metasurface enhances the collection efficiency of the UCNPs [97]. These works demonstrate the potential of non-metal plasmonic structures to enhance UCNP photoluminescence without the quenching usually seen for metal plasmonic nanoparticles and structures.

5. Conclusions

Lanthanide-doped UCNPs have the potential to be applied to a wide array of applications due to their rare ability to convert lower-energy excitation into higher-energy emission. But the incredible potential of UCNPs is severely limited by their inherent low efficiency of energy transfer, and therefore low efficiency of upconversion photoluminescence. One potential solution to overcome this limitation is coupling the UCNPs with plasmonic nanoparticles/nanostructures to enhance their upconversion efficiency. This can occur through two main mechanisms: selectively enhanced emission due to the Purcell effect or broadly enhanced excitation due to enhanced local electric field. The literature focuses mostly on the use of noble-metal nanoparticles to enhance either the excitation or emission of UCNPs, but recent studies have begun to explore the potential of using doped semiconductor nanoparticles, dielectric particles, and hybrid systems, as well as dual-mode enhancement. There are still limitations to overcome, including reducing the non-radiative energy transfer from UCNP to metal, to further enhance the efficiency of upconversion nanoparticles, but the direction of current research shows promise for future opportunities.

Conflict of interest


The authors declare no conflict of interest.

Author details

Caroline Friedersdorf and Hao Jing*
Department of Chemistry and Biochemistry, George Mason University, Fairfax, VA, USA

*Address all correspondence to: hjing2@gmu.edu

IntechOpen

© 2024 The Author(s). Licensee IntechOpen. This chapter is distributed under the terms of the Creative Commons Attribution License (<http://creativecommons.org/licenses/by/3.0>), which permits unrestricted use, distribution, and reproduction in any medium, provided the original work is properly cited. 

References

- [1] Auzel F. Upconversion and anti-stokes processes with f and d ions in solids. *Chemical Reviews*. 2004;**104**:139-174
- [2] Liang G, Wang H, Shi H, et al. Recent progress in the development of upconversion nanomaterials in bioimaging and disease treatment. *Journal of Nanobiotechnology*. 2020;**18**:154
- [3] Wang F, Liu X. Upconversion multicolor fine-tuning: Visible to near-infrared emission from lanthanide-doped NaYF₄ nanoparticles. *Journal of the American Chemical Society*. 2008;**130**:5642-5643
- [4] Chen J, Zhao JX. Upconversion nanomaterials: Synthesis, mechanism, and applications in sensing. *Sensors*. 2012;**12**:2414-2435
- [5] Wang M, Abbineni G, Clevenger A, et al. Upconversion nanoparticles: Synthesis, surface modification, and biological applications. *Nanomedicine: Nanotechnology, Biology and Medicine*. 2011;**7**:710-729
- [6] Wen S, Zhou J, Zheng K, et al. Advances in highly doped upconversion nanoparticles. *Nature Communications*. 2018;**9**:2415
- [7] Wu X, Chen G, Shen J, et al. Upconversion nanoparticles: A versatile solution to multiscale biological imaging. *Bioconjugate Chemistry*. 2015;**26**:166-175
- [8] Xie X, Gao N, Deng R, et al. Mechanistic investigation of photon upconversion in Nd³⁺-sensitized core-shell nanoparticles. *Journal of the American Chemical Society*. 2013;**135**:12608-12611
- [9] Zhang Y, Yu Z, Li J, et al. Ultrasmall-superbright neodymium-upconversion nanoparticles via energy migration manipulation and lattice modification: 808 nm-activated drug release. *ACS Nano*. 2017;**11**:2846-2857
- [10] Xie X, Gao N, Deng R, et al. Mechanistic investigation of photon upconversion in Nd³⁺-sensitized core-shell nanoparticles. *Journal of the American Chemical Society*. 2013;**135**:12608-12611
- [11] Pominova D, Proydakova V, Romanishkin I, et al. NaGdF₄:Yb, Er, Tm upconversion nanoparticles for bioimaging in shortwave-infrared range: Study of energy transfer processes and composition optimization. *Photonics*. 2024;**11**:38
- [12] Qin X, Xu J, Wu Y, et al. Energy-transfer editing in lanthanide-activated upconversion nanocrystals: A toolbox for emerging applications. *ACS Central Science*. 2019;**5**:29-42
- [13] Su Q, Han S, Xie X, et al. The effect of surface coating on energy migration-mediated upconversion. *Journal of the American Chemical Society*. 2012;**134**:20849-20857
- [14] Lee G, Park YI. Lanthanide-doped upconversion nanocarriers for drug and gene delivery. *Nanomaterials*. 2018;**8**:511
- [15] Liu Y, Liang S, Yuan C, et al. Fabrication of anticounterfeiting nanocomposites with multiple security features via integration of a photoresponsive polymer and upconverting nanoparticles. *Advanced Functional Materials*. 2021;**31**:2103908
- [16] Kanodarwala FK, Leśniewski A, Olszowska-Łoś I, et al. Fingerprint detection using upconverting

nanoparticles and comparison with cyanoacrylate fuming. *Forensic Science International*. 2021;**326**:110915

[17] Liu B-T, Huang T-H, Wang T-L, et al. Enhanced efficiency of low-temperature fabricated dye-sensitized solar cells by incorporating upconversion nanoparticles. *Solar Energy*. 2021;**227**:1-7

[18] Chaudhary N, Pahuja M, Ghosh K. Upconversion as a spear carrier for tuning photovoltaic efficiency. *Materials Advances*. 2024;**5**:1783-1802

[19] Li S, Wei X, Li S, et al. Up-conversion luminescent nanoparticles for molecular imaging, cancer diagnosis and treatment. *International Journal of Nanomedicine*. 2020;**15**:9431-9445

[20] Mohanty S, Kaczmarek AM. Unravelling the benefits of transition-metal-co-doping in lanthanide upconversion nanoparticles. *Chemical Society Reviews*. 2022;**51**:6893-6908

[21] Bünzli J-CG, Piguet C. Taking advantage of luminescent lanthanide ions. *Chemical Society Reviews*. 2005;**34**:1048-1077

[22] Dorenbos P. The 5d level positions of the trivalent lanthanides in inorganic compounds. *Journal of Luminescence*. 2000;**91**:155-176

[23] Wu Y, Ang MJY, Sun M, et al. Expanding the toolbox for lanthanide-doped upconversion nanocrystals. *Journal of Physics: Applied Physics*. 2019;**52**:383002

[24] Wang F, Liu X. Recent advances in the chemistry of lanthanide-doped upconversion nanocrystals. *Chemical Society Reviews*. 2009;**38**:976-989

[25] Tiwari SP, Maurya SK, Yadav RS, et al. Future prospects of fluoride based

upconversion nanoparticles for emerging applications in biomedical and energy harvesting. *Journal of Vacuum Science and Technology B*. 2018;**36**:060801

[26] Wang F, Deng R, Wang J, et al. Tuning upconversion through energy migration in core-shell nanoparticles. *Nature Materials*. 2011;**10**:968-973

[27] Sun L-D, Dong H, Zhang P-Z, et al. Upconversion of rare earth nanomaterials. *Annual Review of Physical Chemistry*. 2015;**66**:619-642

[28] Safdar M, Ghazy A, Lastusaari M, et al. Lanthanide-based inorganic-organic hybrid materials for photon-upconversion. *Journal of Materials Chemistry C*. 2020;**8**:6946-6965

[29] Lu D, Mao C, Cho SK, et al. Experimental demonstration of plasmon enhanced energy transfer rate in NaYF₄:Yb³⁺,Er³⁺ upconversion nanoparticles. *Scientific Reports*. 2016;**6**:18894

[30] Willets KA, Van Duyne RP. Localized surface plasmon resonance spectroscopy and sensing. *Annual Review of Physical Chemistry*. 2007;**58**:267-297

[31] Kreibig U, Vollmer M. *Optical Properties of Metal Clusters*. Berlin, Heidelberg: Springer; 1995. DOI: 10.1007/978-3-662-09109-8

[32] Kelly KL, Coronado E, Zhao LL, et al. The optical properties of metal nanoparticles: The influence of size, shape, and dielectric environment. *The Journal of Physical Chemistry. B*. 2003;**107**:668-677

[33] Raether H. *Surface Plasmons on Smooth and Rough Surfaces and on Gratings*. Berlin, Heidelberg: Springer; 1988. DOI: 10.1007/BFb0048317

- [34] Jing H, Zhang L, Wang H. Geometrically tunable optical properties of metal nanoparticles. In: Kumar C, editor. UV-VIS and Photoluminescence Spectroscopy for Nanomaterials Characterization. Berlin, Heidelberg: Springer; 2013. pp. 1-74
- [35] Bohren C, Huffman D. Absorption and Scattering of Light by Small Particles. New York: Wiley; 1998
- [36] Unser S, Bruzas I, He J, et al. Localized surface plasmon resonance biosensing: Current challenges and approaches. *Sensors*. 2015;**15**:15684-15716
- [37] Loiseau A, Asila V, Boitel-Aullen G, et al. Silver-based plasmonic nanoparticles for and their use in biosensing. *Biosensors*. 2019;**9**:78
- [38] Farooq S, Wali F, Zezell DM, et al. Optimizing and quantifying gold nanospheres based on LSPR label-free biosensor for dengue diagnosis. *Polymers*. 2022;**14**:1592
- [39] Farooq S, Rativa D, de Araujo RE. Orientation effects on plasmonic heating of near-infrared colloidal gold nanostructures. *Plasmonics*. 2020;**15**:1507-1515
- [40] Tian F, Bonnier F, Casey A, et al. Surface enhanced Raman scattering with gold nanoparticles: Effect of particle shape. *Analytical Methods*. 2014;**6**:9116-9123
- [41] Kong F-Y, Zhang J-W, Li R-F, et al. Unique roles of gold nanoparticles in drug delivery, targeting and imaging applications. *Molecular Journal of Synthesizer Chem Natural Products Chemistry*. 2017;**22**:1445
- [42] Mie G. Beiträge zur Optik trüber Medien, speziell kolloidaler Metallösungen. *Annalen der Physik*. 1908;**330**:377-445
- [43] Mie G. Contributions to the Optics of Turbid Media, Particularly of Colloidal Metal Solutions. Albuquerque, New Mexico: Technical Translation Service Sandia Laboratories; 1978
- [44] Zheng J, Cheng X, Zhang H, Bai X, Ai R, Shao L, et al. Gold nanorods: The most versatile plasmonic nanoparticles. *Chemical Reviews*. 2021;**121**:13342-13453. DOI: 10.1021/acs.chemrev.1c00422 [Accessed: September 26, 2024]
- [45] Park J-E, Lee Y, Nam J-M. Precisely shaped, uniformly formed gold nanocubes with ultrahigh reproducibility in single-particle scattering and surface-enhanced Raman scattering. *Nano Letters*. 2018;**18**:6475-6482
- [46] Chow TH, Li N, Bai X, et al. Gold nanobipyramids: An emerging and versatile type of plasmonic nanoparticles. *Accounts of Chemical Research*. 2019;**52**:2136-2146
- [47] Stangherlin S, Cathcart N, Sato F, et al. Gold nanoprisms: Synthetic approaches for mastering plasmonic properties and implications for biomedical applications. *ACS Applied Nano Materials*. 2020;**3**:8304-8318
- [48] Fabris L. Gold nanostars in biology and medicine: Understanding physicochemical properties to broaden applicability. *Journal of Physical Chemistry C*. 2020;**124**:26540-26553
- [49] Skrabalak SE, Chen J, Sun Y, et al. Gold nanocages: Synthesis, properties, and applications. *Accounts of Chemical Research*. 2008;**41**:1587-1595
- [50] Fan X, Zheng W, Singh DJ. Light scattering and surface plasmons on small spherical particles. *Light: Science & Applications*. 2014;**3**:e179-e179
- [51] Gérard D, Gray SK. Aluminium plasmonics. *Journal of Physics Applied Physics*. 2014;**48**:184001

- [52] Souri S, Hadilou N, Navid HA, et al. A rational design of multimodal asymmetric nanoshells as efficient tunable absorbers within the biological optical window. *Scientific Reports*. 2021;**11**:15115
- [53] Ershov V, Tarasova N, Ershov B. Evolution of electronic state and properties of silver nanoparticles during their formation in aqueous solution. *International Journal of Molecular Sciences*. 2021;**22**:10673
- [54] Agrawal A, Cho SH, Zandi O, et al. Localized surface plasmon resonance in semiconductor nanocrystals. *Chemical Reviews*. 2018;**118**:3121-3207
- [55] Chen L, Sakamoto M, Sato R, et al. Determination of a localized surface plasmon resonance mode of Cu₇S₄ nanodisks by plasmon coupling. *Faraday Discussions*. 2015;**181**:355-364
- [56] Luther JM, Jain PK, Ewers T, et al. Localized surface plasmon resonances arising from free carriers in doped quantum dots. *Nature Materials*. 2011;**10**:361-366
- [57] Kanehara M, Koike H, Yoshinaga T, et al. Indium tin oxide nanoparticles with compositionally tunable surface plasmon resonance frequencies in the near-IR region. *Journal of the American Chemical Society*. 2009;**131**:17736-17737
- [58] Rowe DJ, Jeong JS, Mkhoyan KA, et al. Phosphorus-doped silicon nanocrystals exhibiting mid-infrared localized surface plasmon resonance. *Nano Letters*. 2013;**13**:1317-1322
- [59] Qin X, Carneiro Neto AN, Longo RL, et al. Surface plasmon-photon coupling in lanthanide-doped nanoparticles. *Journal of Physical Chemistry Letters*. 2021;**12**:1520-1541
- [60] Mendez-Gonzalez D, Melle S, Calderón OG, et al. Control of upconversion luminescence by gold nanoparticle size: From quenching to enhancement. *Nanoscale*. 2019;**11**:13832-13844
- [61] Dong J, Gao W, Han Q, et al. Plasmon-enhanced upconversion photoluminescence: Mechanism and application. *Reviews in Physics*. 2019;**4**:100026
- [62] Purcell EM, Torrey HC, Pound RV. Resonance absorption by nuclear magnetic moments in a solid. *Physics Review*. 1946;**69**:37-38
- [63] Park W, Lu D, Ahn S. Plasmon enhancement of luminescence upconversion. *Chemical Society Reviews*. 2015;**44**:2940-2962
- [64] Das A, Bae K, Park W. Enhancement of upconversion luminescence using photonic nanostructures. *Nano*. 2020;**9**:1359-1371
- [65] Rasskazov IL, Wang L, Murphy CJ, et al. Plasmon-enhanced upconversion: Engineering enhancement and quenching at nano and macro scales. *Optical Materials Express*. 2018;**8**:3787-3804
- [66] Wang L, Guo S, Liu D, et al. Plasmon-enhanced blue upconversion luminescence by indium nanocrystals. *Advanced Functional Materials*. 2019;**29**:1901242
- [67] Yu H, Peng Y, Yang Y, et al. Plasmon-enhanced light-matter interactions and applications. *npj Computational Materials*. 2019;**5**:1-14
- [68] Zhu B, Feng X, Chen L, et al. Simulation of LSPR optical and electric field enhancement distribution based on gold nanobipyramids using a

modified nanosphere. *Materials Today Communications*. 2022;**32**:104136

[69] Liu X, Yuan LD. Simultaneous excitation and emission enhancements in upconversion luminescence using plasmonic double-resonant gold nanorods. *Scientific Reports*. 2015;**5**:15235

[70] Fischer S, Hallermann F, Eichelkraut T, et al. Plasmon enhanced upconversion luminescence near gold nanoparticles–simulation and analysis of the interactions. *Optics Express*. 2012;**20**:271

[71] Clarke C, Liu D, Wang F, et al. Large-scale dewetting assembly of gold nanoparticles for plasmonic enhanced upconversion nanoparticles. *Nanoscale*. 2018;**10**:6270-6276

[72] Gao W, Han S, Wang B, et al. Single-layer gold nanoparticle film enhances the upconversion luminescence of a single NaYbF₄: 2%Er³⁺ microdisk. *Journal of Alloys and Compounds*. 2022;**900**:163493

[73] Das A, Mao C, Cho S, et al. Over 1000-fold enhancement of upconversion luminescence using water-dispersible metal-insulator-metal nanostructures. *Nature Communications*. 2018;**9**:4828

[74] Priyam A, Idris NM, Zhang Y. Gold nanoshell coated NaYF₄ nanoparticles for simultaneously enhanced upconversion fluorescence and darkfield imaging. *Journal of Materials Chemistry*. 2011;**22**:960-965

[75] Liu W, Yang T, Cao K, et al. High-efficiency upconversion luminescence in UCNPs/CsPbBr₃ nanocomposites enhanced by silver nanoparticles. *Optics Letters*. 2024;**49**:1141-1144

[76] Wu Y, Shen X, Dai S, et al. Silver nanoparticles enhanced upconversion

luminescence in Er³⁺/Yb³⁺ codoped bismuth-germanate glasses. *Journal of Physical Chemistry C*. 2011;**115**:25040-25045

[77] Maurya SK, Tiwari SP, Kumar A, et al. Plasmonic enhancement of upconversion emission in Ag@NaYF₄:Er³⁺/Yb³⁺ phosphor. *Journal of Rare Earths*. 2018;**36**:903-910

[78] Lu D, Cho SK, Ahn S, et al. Plasmon enhancement mechanism for the upconversion processes in NaYF₄:Yb³⁺,Er³⁺ nanoparticles: Maxwell versus Förster. *ACS Nano*. 2014;**8**:7780-7792

[79] Li Y, Zeng Y, Su X, et al. Extraordinary upconversion enhancement in mono-dispersed plasmonic resonant nanocavity coupling with lanthanide doped upconversion nanoparticles. *Optics Communication*. 2023;**542**:129599

[80] Reza Dousti M, Amjad RJ. Effect of silver nanoparticles on the upconversion and near-infrared emissions of Er³⁺:Yb³⁺ co-doped zinc tellurite glasses. *Measurement*. 2017;**105**:114-119

[81] Ji Y, Xu W, Li D, et al. Semiconductor plasmon enhanced monolayer upconversion nanoparticles for high performance narrowband near-infrared photodetection. *Nano Energy*. 2019;**61**:211-220

[82] Zhang W, Huang X, Liu W, et al. Semiconductor plasmon enhanced upconversion toward a flexible temperature sensor. *ACS Applied Materials & Interfaces*. 2023;**15**:4469-4476

[83] Zhou D, Liu D, Jin J, et al. Semiconductor plasmon-sensitized broadband upconversion and its enhancement effect on the power

conversion efficiency of perovskite solar cells. *Journal of Materials Chemistry A*. 2017;5:16559-16567

[84] Xia H, Li D, Shang J, et al. Electrically sensitive plasmonic photonic crystals for dynamic upconversion manipulation. *Advanced Functional Materials*. 2023;33:2304045

[85] Maccaferri N, Barbillon G, Koya AN, et al. Recent advances in plasmonic nanocavities for single-molecule spectroscopy. *Nanoscale Advances*. 2021;3:633-642

[86] Nucara L, Greco F, Mattoli V. Electrically responsive photonic crystals: A review. *Journal of Materials Chemistry C*. 2015;3:8449-8467

[87] Liu J, Nero M, Jansson K, et al. Photonic crystals with rainbow colors by centrifugation-assisted assembly of colloidal lignin nanoparticles. *Nature Communications*. 2023;14:3099

[88] Ebbesen TW, Lezec HJ, Ghaemi HF, et al. Extraordinary optical transmission through sub-wavelength hole arrays. *Nature*. 1998;391:667-669

[89] Saboktakin M, Ye X, Chettiar UK, et al. Plasmonic enhancement of nanophosphor upconversion luminescence in Au nanohole arrays. *ACS Nano*. 2013;7:7186-7192

[90] Yin Z, Zhou D, Xu W, et al. Plasmon-enhanced upconversion luminescence on vertically aligned gold nanorod monolayer supercrystals. *ACS Applied Materials & Interfaces*. 2016;8:11667-11674

[91] Lakowicz JR. Radiative decay engineering 5: Metal-enhanced fluorescence and plasmon emission. *Analytical Biochemistry*. 2005;337:171-194

[92] Xu W, Lee TK, Moon B-S, et al. Broadband plasmonic antenna enhanced upconversion and its application in flexible fingerprint identification. *Advanced Optical Materials*. 2018;6:1701119

[93] Chen H, Jiang Z, Hu H, et al. Sub-50-ns ultrafast upconversion luminescence of a rare-earth-doped nanoparticle. *Nature Photonics*. 2022;16:651-657

[94] Mi X, Zhao X, Ji M, et al. Twinned-Au-tip-induced growth of plasmonic Au-Cu Janus nanojellyfish in upconversion luminescence enhancement. *Journal of Colloid and Interface Science*. 2022;624:196-203

[95] de Gennes PG. Soft matter. *Science*. 1992;256:495-497

[96] Zhang X, Fu Q, Duan H, et al. Janus nanoparticles: From fabrication to (bio)applications. *ACS Nano*. 2021;15:6147-6191

[97] Gong C, Liu W, He N, et al. Upconversion enhancement by a dual-resonance all-dielectric metasurface. *Nanoscale*. 2019;11:1856-1862

[98] Liang L, Teh DBL, Dinh N-D, et al. Upconversion amplification through dielectric superlensing modulation. *Nature Communications*. 2019;10:1391

[99] Baranov DG, Zuev DA, Lepeshov SI, et al. All-dielectric nanophotonics: The quest for better materials and fabrication techniques. *Optica*. 2017;4:814-825